HOKKAIDO UNIVERSITY

Title	Exogenous Expression of Equine MHC Class I Molecules in Mice Increases Susceptibility to Equine Herpesvirus 1 Pulmonary Infection
Author(s)	Minato, Erina; Aoshima, Keisuke; Kobayashi, Atsushi et al.
Citation	Veterinary pathology, 56(5), 703-710 https://doi.org/10.1177/0300985819834616
Issue Date	2019-09
Doc URL	https://hdl.handle.net/2115/76630
Rights	Erina Minato, Keisuke Aoshima, Atsushi Kobayashi, Naomi Ohnishi, Nobuya Sasaki, Takashi Kimura, Exogenous Expression of Equine MHC Class I Molecules in Mice Increases Susceptibility to Equine Herpesvirus 1 Pulmonary Infection, Veterinary Pathology (Vol 56 Issue 5, 2019) pp. 703-710. Copyright © 2019 (The Authors). DOI: 10.1177/0300985819834616.
Type	journal article
File Information	manuscript.pdf

Hokkaido University Collection of Scholarly and Academic Papers : HUSCAP

Exogenous expression of equine MHC class I molecules in mice increases susceptibility to equine herpesvirus-1 pulmonary infection

Erina MINATO[1)], Keisuke AOSHIMA[1)], Atsushi KOBAYASHI[1)], Naomi OHNISHI[2)], Nobuya SASAKI[3)], Takashi KIMURA[1)*]

[1)] Laboratory of Comparative Pathology, Faculty of Veterinary Medicine, Hokkaido University, Sapporo, Hokkaido 060-0818, Japan (EM, KA, AK, TK).

[2)] Project for Personalized Cancer medicine, Cancer Precision Medicine Center, Japanese Foundation for Cancer Research, 3-8-31 Ariake, Koto-ku, Tokyo, 135-8550, Japan (NO).

[3)] Laboratory of Laboratory Animal Science and Medicine, School of Veterinary Medicine, Kitasato University, Towada, Japan (NS).

*Correspondence to: T. Kimura, Laboratory of Comparative Pathology, Faculty of Veterinary Medicine, Hokkaido University, Sapporo, Hokkaido 060-0818, Japan.

E-mail: tkimura@vetmed.hokudai.ac.jp

Tel: +81-11-706-5191; Fax: +81-11-706-5194

Running head: TRANSGENIC MICE EXPRESSING EHV-1 RECEPTOR

Abstract

Equine herpesvirus-1 (EHV-1) utilizes equine major histocompatibility complex class I (MHC class I) as an entry receptor. Exogenous expression of equine MHC class I genes in murine cell lines confers susceptibility to EHV-1 infection. In order to examine the *in vivo* role of equine MHC class I as an entry receptor for EHV-1, we generated transgenic (Tg) mice expressing equine MHC class I under the control of the CAG promoter. Equine MHC class I protein was expressed in the liver, spleen, lung, and brain of Tg mice, which was confirmed by western blot. However, equine MHC class I antigen was only detected in bronchiolar epithelium and not in other tissues, using the immunofluorescence method employed in this study. Both Tg and wild-type (WT) mice developed pneumonia 3 days after intranasal infection with EHV-1. The bronchiolar epithelial cells of Tg mice showed severer necrosis, compared with those in WT mice. In addition to this, the number of virus antigen-positive cells in the lungs was higher in Tg mice than in WT mice. These results suggest that exogenous expression of equine MHC class I renders mice more susceptible to EHV-1 infection.

KEY WORDS: Equine herpesvirus-1, MHC class I, transgenic mice, horses, respiratory diseases, nervous system diseases

Equine herpesvirus-1 (EHV-1) causes respiratory disease, abortion, and encephalomyelitis. In horses, following oronasal transmission, EHV-1 infection occurs in respiratory epithelial cells and local lymph nodes [9,12]. This results in a leukocyte-associated viremia, followed by the infection of endothelial cells in the pregnant uterus and central nervous system (CNS) [13]. The pathologic consequences of endothelial infection in the uterus and CNS are vasculitis, thrombosis and secondary ischemia that cause abortion [22] and neurological signs [4], respectively. EHV-1 establishes latent infection in T lymphocytes [25] and/or in trigeminal ganglia [21].

Large amounts of experimental data has been generated from infection studies using horses [10,11,27]; however, these studies are labor-intensive. In addition, there are difficulties in obtaining large numbers of horses for experiments. Mice have also been used as models of EHV-1 infection. EHV-1 infected mice are reported to show pneumonia, viremia [2], abortion [1], and viral latency [5]. But, neither viral replication in the endothelial cells nor the subsequent formation of CNS lesion has been reported in the murine model. Equine brain microvascular endothelial cells (EBMECs) are susceptible to EHV-1 infection, whereas their murine counterparts (MEMECs) are EHV-1 resistant, reflecting the inability of the virus to enter mouse cells [7].

Equine major histocompatibility class I (equine MHC class I) is reported to be an entry receptor for EHV-1 [17,18], while EHV-1 is unlikely to utilize mouse MHC class I as a receptor for entry into murine cells. Mouse NIH3T3 cells, which express mouse MHC class I molecules (haplotype $H2^q$) [8,20] on their surface, are not susceptible to EHV-1 infection. However, exogenous expression of equine MHC class I genes in NIH3T3 cells confers susceptibility to EHV-1 infection [18]. These results indicate that MHC class I is one of the determinants underlying species-related differences in the susceptibility to EHV-1.

In the current study, we generated transgenic mice (Tg mice) expressing equine MHC class I to verify its ability to act as an entry receptor for EHV-1 *in vivo* and make mice more susceptible to EHV-1 infection. After inoculation with EHV-1,

we compared the histopathological changes in Tg mice with those in their wild−type (WT) littermates to evaluate the effect of equine MHC class I expression on EHV-1 pathogenicity.

MATERIALS AND METHODS

Virus

The EHV-1 strain Ab4 [15] was kindly provided by Dr. Hideto Fukushi (Gifu University, Gifu, Japan). Stock viruses were cultured in rabbit kidney (RK13) cells, and titrated by plaque formation assays on RK13 cells.

Plasmid

The plasmid vector pCXSN was generated as previously described [18]. The plasmid pCAGGS-MCS(KS), which was kindly provided by Dr. Naomi Ohnishi (Japanese Foundation for Cancer Research, Tokyo, Japan), was generated from pCAGGS [14] by replacing the cloning site with *Kpn*I, *Xho*I, *Eco*RI, and *Sac*I endonuclease recognition sequences.

Tg mice

DNA fragments of equine MHC class I heavy chain A68 (GenBank/EMBL/DDBJ entry AB525079) excised from pCXSN-A68-HA [18] were cloned into the *Xho*I-*Hind*III site of a pSP73 vector (Promega, USA) to generate vector pSP-A68. Construction of pSP-V5 68 was done by the insertion of a V5 epitope tag following the putative signal alignment of A68 into the pSP-A68 vector using inverse polymerase chain reaction (PCR). The region of DNA containing the equine β2-microglobulin (β2m) was amplified by PCR from plasmid pCXSN-equine β2m [18], and cloned into the *Hind*III-*Eco*RI site of pSP-V5 68 (pSP-V68-B2M). To induce bicistronic expression of the equine MHC class I heavy chain A68 and equine β2m on the cell surface, 2A oligopeptide (ATNFSLLKQAGDVEENPGP) [24] was inserted between the C terminus of A68 and the N terminus of β2M in pSP-V68-B2M

using inverse PCR (pSP-V68-2A-B2M). The V68-2A-B2M fragment was then excised as an *Xho*I-*Eco*RI fragment, and cloned into vector pCAGGS-MCS(KS) to generate the vector pCAGGS-V68-2A-B2M. The equine MHC class I heavy chain A68 with equine β2m excised from pCAGGS-V68-2A-B2M as a *Sna*BI-*Hind*III fragment was used as a transgene (Fig. 1). The transgene was microinjected into fertilized eggs of Slc:BDF1 mice (Japan SLC,Inc.). The transgenic founders carrying the *A68* gene were backcrossed with BALB/cAJcl (CLEA Japan, Inc.). The mouse line designated BALB/cAJcl;BDF1-Tg (CAG-Eq-MHC-I-B2M) 30LCP/A68 was used in this study as Tg mice.

Genotyping of Tg mice

The founder and its progeny were genotyped by PCR. Mouse tail-derived DNA was used as template. PCR was performed with 2 × Quick Taq HS DyeMix (TOYOBO, Japan), 0.2 μM each of the primers, and 200 ng of DNA. Details of the PCR primers used for amplification are shown in Table 1. For amplification of the *A68* gene, primers A68-B2M-F1 and PCAGGS-REV were used; for amplification of mouse actin, primers mouse actin F and mouse actin R were used. The PCR cycling profile was 94 °C for 2 min for denaturation, followed by 35 sequential cycles of 94 °C for 30 s, 63 °C for 30 s, and 72 °C for 1 min. The PCR products were electrophoretically analyzed on 1.5% agarose gels.

Reverse transcription-polymerase chain reaction (RT-PCR)

The liver, spleen, kidney, and lung of Tg mice were collected. Total RNA was extracted using TRIZOL reagent (Thermo Fisher Scientific, USA). The RNA samples were treated with DNase I, Amplification Grade (Thermo Fisher Scientific) to digest contaminating DNA. Synthesis of complementary DNA (cDNA) was carried out using the SuperScript™ III First-Strand Synthesis System (Thermo Fisher Scientific). PCR was performed with 0.2 mM dNTP, 10 × PCR buffer, 1.5 mM $MgCl_2$, 1.25 units of HotStarTaq DNA Polymerase (Qiagen, Germany), 0.3 μM of each primer, and 1 μl of

cDNA in a total volume of 12.5 μl. The PCR primers used for amplification were the same as those used in genotyping of Tg mice. The PCR cycling profile was 95 °C for 15 min for initial denaturation; followed by 40 sequential cycles of 94 °C for 30 s, 63 °C for 1 min, and 72 °C for 1 min; and final extension at 72 °C for 10 min. The PCR products were electrophoretically analyzed on 1.5% agarose gels.

Western Blot

The liver, spleen, lung, and brain of Tg mice or WT mice were collected. The tissues were lysed in lysis buffer (10 mM Tris-HCl, pH 7.5; 150 mM $NaCl_2$; 5 mM EDTA; 10% glycerol; and 1% Triton X-100) supplemented with complete protease inhibitor cocktail (Sigma-Aldrich, USA). Lysed proteins were homogenized and sonicated. Following sodium dodecyl sulfate polyacrylamide gel electrophoresis (SDS-PAGE), proteins were transferred onto Immobilon-P transfer membranes (Merck Millipore, USA), and labeled with anti-V5 antibody (Thermo Fisher Scientific), or anti-actin antibody clone C4 (Merck Millipore).

Immunofluorescence staining

The lungs of Tg mice or WT mice were collected, and the tissues were fixed in 4% paraformaldehyde/phosphate-buffered saline (PBS). The tissues were paraffin-embedded, and sections were prepared using standard methods. Indirect immunofluorescence staining was performed using Tyramide SuperBoost kits with Alexa Fluor Tyramides (Thermo Fisher Scientific). Briefly, the sections were deparaffinized, heated with 0.01 M citric acid buffer (pH 6.0) using a microwave for antigen retrieval, treated with 0.3% hydrogen peroxide in methanol, and blocked with 10% normal rabbit serum. A goat anti-V5-tag polyclonal antibody (ab95038; Abcam, England) was added, and the sections were incubated overnight at 4 °C. The sections were then washed with PBS, and incubated with donkey anti-goat horseradish peroxidase (HRP)-conjugated IgG (Santa Cruz Biotechnology, USA) for 20 min at room temperature. After further washing with PBS, the sections were

incubated with Alexa Fluor 488 Tyramide Reagent for 10 min at room temperature. Nuclei were stained with Hoechst 33258 (Sigma-Aldrich). As a negative control, sections were stained without primary antibody. The fluorescent-stained sections were examined using an LSM 700 confocal microscope (Zeiss, Germany).

Experimental infection

Heterozygous Tg mice and WT littermate mice were used at six weeks of age. Seven Tg mice and three WT mice were anesthetized with isoflurane, and intranasally inoculated with 2×10^6 plaque forming units (PFU) of EHV-1 Ab4. All animal experiments were authorized by the Institutional Animal Care and Use Committee of the Graduate School of Veterinary Medicine, Hokkaido University (approval number: 13-0092), and all experiments were performed according to the guidelines of this committee.

Histopathology and Immunohistochemistry

The mice inoculated with EHV-1 were euthanized and necropsied at 3 d post-inoculation (p.i.). The liver, spleen, kidneys, heart, lung, and brain were collected. All organs were fixed with 4% paraformaldehyde/PBS. The tissues were paraffin-embedded, sectioned at 2 to 4 μm, and stained with hematoxylin and eosin (HE). To calculate the number of necrotic bronchiolar epithelial cells in the lungs, total number of bronchiolar epithelial cells showing necrotic morphology in each section and the total area of the sections was measured using a CellSens Dimension microscope (Olympus, Japan). The number of necrotic cells was divided by the total area of each section. The mean number of necrotic cells in the bronchioles of Tg mice was compared with those of WT mice using the Welch two-sample t-test.

Indirect immunohistochemistry staining was carried out using the labeled streptavidin-biotin (SAB) technique (Histofine SAB-PO Kit, Nichirei, Japan). Briefly, the sections were deparaffinized, heated with 0.01 M citric acid buffer (pH 6.0) using a microwave for antigen retrieval, treated with 0.3% hydrogen peroxide in methanol,

and blocked with 10% normal rabbit serum. Goat anti-equine rhinopneumonitis virus/equine herpesvirus type 1 polyclonal antiserum (VMRD, USA) or polyclonal rabbit anti-human CD3 antibody (Agilent, USA) was added, and the sections were incubated overnight at 4 ºC. The sections were then washed with PBS, and incubated with a secondary antibody labeled with biotin for 20 min at room temperature. After additional washing with PBS, the sections were incubated with peroxidase-conjugated streptavidin for 10 min at room temperature. The bound peroxidase was detected with 3,3'-diaminobenzidine (DAB). The sections were counterstained with hematoxylin. As a negative control, sections were stained without primary antibody.

To calculate the number of cells in the lungs that were positive for viral antigen, the total number of EHV-1-positive cells were counted in each section of the tissue and the total area of the sections was measured using a CellSens Dimension microscope . The number of positive cells was divided by the total area of each section. The mean number of EHV-1-positive cells in the lungs of Tg mice was compared with the number in the lungs of WT mice using the Welch two-sample t-test.

To calculate the number of T cells in the lung, CD3-positive cells were counted in each tissue section using ImageJ[19]. The number of positive cells was divided by the total area of each section. The mean number of CD3-positive cells was statistically compared in Tg and WT mice by using the Mann-Whitney U test.

RESULTS

Tg mice expressing equine MHC class I

Tg mice expressing equine MHC class I were generated as described in the Materials and Methods. Because endogenous MHC class I is expressed on most somatic cells [3], we used the CAG promoter, which can induce ubiquitous gene expression (Fig. 1) [14]. Expression of equine MHC class I heavy chain mRNA and protein was detected in the heterozygous Tg mice, but not in the WT littermate mice

(Fig. 2, 3). The level of equine MHC class I protein in the brain was lower than in the liver, spleen, and lung (Fig. 3). Immunofluorescence staining revealed the expression of equine MHC class I on the apical surface of bronchiolar epithelial cells of the Tg, but not of the WT mice (Fig. 4, 5). Expression of equine MHC class I was not detected by immunofluorescence staining in the liver, spleen, kidney, heart, or brain of either Tg or WT mice.

Experimental infection

Starting at 1d p.i., all EHV-1-inoculated mice, Tg and WT, began to show tachypnea and lethargy with ruffled fur. At 3 d p.i., all mice inoculated with EHV-1 had postmortem lesions of bronchointerstitial pneumonia, with peribronchiolar, and perivascular infiltration of lymphocytes, macrophages, and neutrophils. Necrosis of the bronchiolar epithelial cells were more evident in Tg mice than in WT mice (Figs. 6a, 8a and 10; $p < 0.05$). Using IHC, we detected EHV-1 in the nucleus and cytoplasm of bronchiolar epithelial cells and macrophages in both groups of mice (Figs. 6b, 8b, Supplemental Figures S1 and S2). More EHV-1-positive cells were found in the lungs of Tg mice than those of WT mice (Fig.11; $p < 0.05$). Furthermore, perivascular edema was much more prominent in the Tg mice; however, virus antigen was not detected in the vascular endothelium (Fig. 7a, 7b, 9a and 9b). Inflammatory cells infiltrating the lung were primarily lymphocytes. The number of CD3-positive cells in the lung did not differ between the two groups of mice (Fig.12; $p > 0.05$). Notably, neither histological lesions nor viral antigen were detected in the liver, spleen, kidneys, heart, and brain of Tg or WT mice inoculated with EHV-1.

DISCUSSION

We generated Tg mice expressing equine MHC class I molecules, which are known to act as entry receptors for EHV-1 *in vitro*. Western blot analysis showed the expression of equine MHC class I proteins in various organs including the lung. After

experimental nasal infection with EHV-1, the number of EHV-1-infected cells observed in the lung of Tg mice was higher than in that of WT mice. These results suggest that exogenous expression of equine MHC class I increased the susceptibility of mice to EHV-1 infection.

Intranasal infection with EHV-1 in adult BALB/c mice causes bronchiolar epithelial infection as well as pulmonary lesions with intranuclear inclusions and peribronchiolar and perivascular mononuclear cell infiltrates [2]. Our mice developed similar lesions upon EHV-1 intranasal infection. However, infection and necrosis of the bronchiolar epithelium were severer in Tg mice expressing equine MHC class I compared to the WT mice. This finding was consistent with the result of immunofluorescent staining that revealed selective expression of equine MHC class I expression in the bronchiolar epithelium of Tg mice.

Perivascular edema surrounding pulmonary arteries was a characteristic lesion in both Tg and WT mice, but was more severe in Tg mice than WT mice. Because neither vascular endothelial cells nor vascular smooth muscle cells were positive for viral antigen, the edema may have reflected the severity of adjacent bronchiolar damage.

The role of leukocytes in lung lesion pathogenesis remains unclear. The numbers of CD3-positive cells in the lung were similar in WT and Tg mice, although necrosis and desquamation of bronchiolar epithelial cells were more evident in the Tg mice. Foals infected with EHV-1 show necrotizing bronchiolitis and infiltration of mononuclear cells [6,26] similar to the lesions of the Tg mice in this study. Smith *et al.* previously reported that mice infected with EHV-1 RacL11 strain developed more severe lung lesions than those infected with attenuated KyA strain [23]. Interestingly, the level of proinflammatory beta chemokines produced in the bronchiolar lavage fluid by RacL11 was higher than that by KyA, despite identical T cell responses and

viral loads in the lungs of both strains [23]. Therefore, pathogenesis of the relatively severe lung lesions in EHV-1 in Tg mice may involve a contribution of the immune response in addition to a direct cytolytic effect of the viral infection.

Immunofluorescence staining of the V5 epitope tag did not show positivity in the liver, spleen, and brain of Tg mouse, although RT-PCR and western blot analyses demonstrated the gene and protein expression of equine MHC class I in these organs. It may be that expression levels of equine MHC class I in cell types other than bronchiolar epithelial cells were below the detection limit of the indirect immunofluorescent technique. The CAG promoter used in this study is known to induce high-level gene expression in mammalian cells; however, at times it fails to attain sufficient protein expression levels, depending on the nature of the cargo gene and/or the type of host cell [16]. An unknown mechanism was potentially involved in determining the final stationary expression levels of the equine MHC class I in the mice.

Neither histological lesions nor viral antigens were detected in the liver, spleen, kidneys, heart and brain of the Tg mouse at 3d after intranasal inoculation with EHV-1. This was consistent with the paucity of equine MHC class I antigen-specific signal obtained in these tissues by immunofluorescent staining. Notably, western blot analysis showed the expression of exogenous protein in all examined organs, albeit at levels below the detection limit of immunofluorescent staining. Therefore, it will be interesting to investigate the susceptibility of Tg mice to EHV-1 by using alternative routes of virus inoculation.

This study suggests that transgenic expression of equine MHC class I is a useful method for increasing the *in vivo* susceptibility of mouse cells to EHV-1 infection. New Tg mice with more widespread overexpression of equine MHC class I, including additional EHV-1 target cells (e.g. endothelial cells and leukocytes) in

addition to bronchiolar epithelial cells may provide a suitable model for the study of EHV-1 pathogenesis.

ACKNOWLEDGMENTS

This work was supported by Grant-in-Aid for Scientific Research (B) from the Ministry of Education, Culture, Sports, Science, and Technology, Japan.

REFERENCES

1. Awan AR, Baxi M, Field HJ. EHV-1-induced abortion in mice and its relationship to stage of gestation. *Res Vet Sci*. 1995 Sep;59:139–145.
2. Awan AR, Chong YC, Field HJ. The pathogenesis of equine herpesvirus type 1 in the mouse: a new model for studying host responses to the infection. *J Gen Virol*. 1990;71:1131–1140.
3. David-Watine B, Israël A, Kourilsky P. The regulation and expression of MHC class I genes. *Immunol Today*. 1990 Aug;11:286–292.
4. Edington N, Bridges CG, Patel JR. Endothelial cell infection and thrombosis in paralysis caused by equid herpesvirus-1: equine stroke. *Arch Virol*. 1986;90:111–124.
5. Field HJ, Awan AR. Reinfection and reactivation of equine herpesvirus-1 in the mouse. *Arch Virol*. 1992;123:409–419.
6. HARTLEY WJ, DIXON RJ. An outbreak of Foal Perinatal Mortality due to Equid Herpesvirus Type I: Pathological Observations. *Equine Vet J*. 1979;11:215–218.
7. Hasebe R, Kimura T, Nakamura K, et al. Differential susceptibility of equine and mouse brain microvascular endothelial cells to equine herpesvirus 1 infection. *Arch Virol*. 2006 Apr 3;151:775–786.
8. Herrmann F, Lehr H-A, Drexler I, et al. HER-2/neu-mediated regulation of

components of the MHC class I antigen-processing pathway. *Cancer Res*. 2004 Jan 1;64:215–220.

9. Kydd JH, Smith KC, Hannant D, Livesay GJ, Mumford JA. Distribution of equid herpesvirus-1 (EHV-1) in respiratory tract associated lymphoid tissue: implications for cellular immunity. *Equine Vet J*. 1994 Nov;26:470–473.

10. Laval K, Favoreel HW, Poelaert KC, Van Cleemput J, Nauwynck HJ. Equine Herpesvirus Type 1 Enhances Viral Replication in CD172a+ Monocytic Cells upon Adhesion to Endothelial Cells. *J Virol*. 2015;89:10912–10923.

11. Laval K, Favoreel HW, Nauwynck HJ. Equine herpesvirus type 1 replication is delayed in CD172a + monocytic cells and controlled by histone deacetylases. *J Gen Virol*. 2015;118–130.

12. Lunn DP, Davis-Poynter N, Flaminio MJBF, et al. Equine herpesvirus-1 consensus statement. *J Vet Intern Med*. 2009;23:450–461.

13. Ma G, Azab W, Osterrieder N. Equine herpesviruses type 1 (EHV-1) and 4 (EHV-4)-Masters of co-evolution and a constant threat to equids and beyond. *Vet Microbiol*. 2013;167:123–134.

14. Niwa H, Yamamura K, Miyazaki J. Efficient selection for high-expression transfectants with a novel eukaryotic vector. *Gene*. 1991 Dec 15;108:193–199.

15. Nugent J, Birch-Machin I, Smith KC, et al. Analysis of Equid Herpesvirus 1 Strain Variation Reveals a Point Mutation of the DNA Polymerase Strongly Associated with Neuropathogenic versus Nonneuropathogenic Disease Outbreaks. *J Virol*. 2006 Apr 15;80:4047–4060.

16. Sakaguchi M, Watanabe M, Kinoshita R, et al. Dramatic increase in expression of a transgene by insertion of promoters downstream of the cargo gene. *Mol Biotechnol*. 2014 Jul;56:621–630.

17. Sasaki M, Kim E, Igarashi M, et al. Single Amino Acid Residue in the A2 Domain of Major Histocompatibility Complex Class I Is Involved in the Efficiency of Equine Herpesvirus-1 Entry. *J Biol Chem*. 2011 Nov 11;286:39370–39378.

18. Sasaki M, Hasebe R, Makino Y, et al. Equine major histocompatibility complex class I molecules act as entry receptors that bind to equine herpesvirus-1 glycoprotein D. *Genes to Cells*. 2011 Apr;16:343–357.
19. Schneider CA, Rasband WS, Eliceiri KW. NIH Image to ImageJ: 25 years of image analysis. *Nat Methods*. 2012 Jul;9:671–675.
20. Seliger B, Harders C, Lohmann S, et al. Down-regulation of the MHC class I antigen-processing machinery after oncogenic transformation of murine fibroblasts. *Eur J Immunol*. 1998 Jan;28:122–133.
21. Slater JD, Borchers K, Thackray AM, Field HJ. The trigeminal ganglion is a location for equine herpesvirus 1 latency and reactivation in the horse. *J Gen Virol*. 1994;75:2007–2016.
22. Smith KC, Whitwell KE, Mumford JA, Gower SM, Hannant D, Tearle JP. An immunohistological study of the uterus of mares following experimental infection by equid herpesvirus 1. *Equine Vet J*. 1993 Jan;25:36–40.
23. Smith PM, Zhang Y, Grafton WD, Jennings SR, O'Callaghan DJ. Severe murine lung immunopathology elicited by the pathogenic equine herpesvirus 1 strain RacL11 correlates with early production of macrophage inflammatory proteins 1alpha, 1beta, and 2 and tumor necrosis factor alpha. *J Virol*. 2000;74:10034–10040.
24. Szymczak AL, Workman CJ, Wang Y, et al. Correction of multi-gene deficiency in vivo using a single "self-cleaving" 2A peptide-based retroviral vector. *Nat Biotechnol*. 2004 May 4;22:589–594.
25. Welch HM, Bridges CG, Lyon AM, Griffiths L, Edington N. Latent equid herpesviruses 1 and 4: detection and distinction using the polymerase chain reaction and co-cultivation from lymphoid tissues. *J Gen Virol*. 1992 Feb 1;73:261–268.
26. Whitwell, K. E. and ASB. Pathological findings in horses dying during an outbreak of the paralytic form of equid herpesvirus type 1(EHV-1) infection. *Equine Vet J*. 1992;24:13–19.

27. Wilsterman S, Soboll-Hussey G, Lunn DP, et al. Equine herpesvirus-1 infected peripheral blood mononuclear cell subpopulations during viremia. *Vet Microbiol*. 2011;149:40–47.

FIGURE LEGENDS

Figure 1. Design of the transgene construct used to generate transgenic mice expressing equine MHC class I. V5: gene coding for the V5 epitope tag. 2A: gene coding for the 2A peptide; self-cleavage occurs in the 2A peptide following translation. The arrows indicate the position of the primers (A68-B2M-F and PCAGGS-REV) used in PCR genotyping to detect exogenous expression of equine MHC class I.

Figures 2–3. Exogenous expression of equine MHC class I in the liver, spleen, lung, and brain of transgenic (Tg) mice, but not in the lung of wild-type (WT) littermate mice. **Figure 2.** Expression of equine MHC class I mRNA detected by RT-PCR. Actin was used as an internal control. **Figure 3.** Expression of equine MHC class I protein detected by western blot analysis using an anti-V5 antibody. Actin was used as an internal control. A non-specific band with a higher molecular weight was observed in the panel of the WT lung.

Figures 4–5. Exogenous expression of equine MHC class I, lung, mice. Immunofluorescent staining using an anti-V5 antibody (green). **Figure 4.** Bronchiolar epithelial cells of transgenic mice were positive for equine MHC class I. **Figure 5.** Equine MHC class I was not expressed in the bronchiolar epithelial cells from wild-type littermate mice.

Figures 6–7. Equine herpesvirus 1 (EHV-1) infection, lung, mice transgenic for equine MHC class I . **Figure 6.** (a) Necrosis and desquamation of bronchiolar epithelial cells. Remaining bronchiolar epithelial cells often showed degeneration. Arrowheads indicate desquamated epithelial cells. HE. (b) EHV-1 antigen was detected in most desquamated epithelial cells. Immunohistochemistry (IHC) for EHV-

1. **Figure 7.** (a) Perivascular edema. HE. (b) EHV-1 antigen was not detected in vascular endothelial cells. A bronchiole with positive immunolabelling is present at lower left. IHC for EHV-1 antigen.

Figures 8–9. Equine herpesvirus 1 (EHV-1) infection, lung, wild type littermate mice. **Figure 8.** (a) Necrosis of few bronchiolar epithelial cells. Arrowheads indicate desquamated epithelial cells. HE. (b) Sporadic EHV-1 antigen was detected in the epithelial cells. Immunohistochemistry (IHC) for EHV-1 antigen. **Figure 9.** (a) Mild perivascular edema. HE. (b) Vascular endothelial cells were negative for the EHV-1 antigen. A bronchiole with positive immunolabelling is present at right. IHC for EHV-1 antigen.

Figure 10. Number of necrotic bronchiolar epithelial cells within lungs. Error bars show standard deviations. *p = 0.01895, Welch two sample t-test, n=7 for transgenic (Tg) mice (mean ± SD = 1.72 ± 1.064 × 10^{-5} cells / μm^2), n=3 for wild type (WT) mice (0.452 ± 0.141 × 10^{-5} cells / μm^2).

Figure 11. Number of EHV-1 antigen-positive cells within lung. Error bars show standard deviations. *p = 0.04109, Welch two sample t-test, n= 7 for transgenic (Tg) mice (mean ± SD = 12 ± 3.00 × 10^{-5} cells / μm^2), n= 3 for wild type (WT) mice (4.84 ± 3.38 × 10^{-5} cells / μm^2).

Figure 12. Number of CD3-positive cells within lung tissues. Error bars represent standard deviation. p = 0.3677, Mann-Whitney U test, n=7 for transgenic (Tg) mice (mean ± SD = 1.69 ± 1.28 × 10^{-5} cells / μm^2), n=3 for wild-type (WT) mice (1.01 ± 0.89 × 10^{-5} cells / μm^2).

1

CAG
promoter
Equine MHC class I
heavy chain A68 gene
Equine β2m
gene
V5
2A
A68B2M-F1
PCAGGS-REV
CAGGS-V68-2A-B2M
3.45 kbp

2

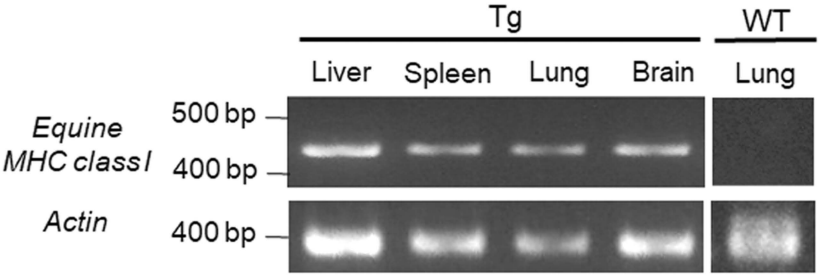
Tg
WT
Liver
Spleen
Lung
Brain
Lung
Equine
MHC class I
500 bp
400 bp
Actin
400 bp

3

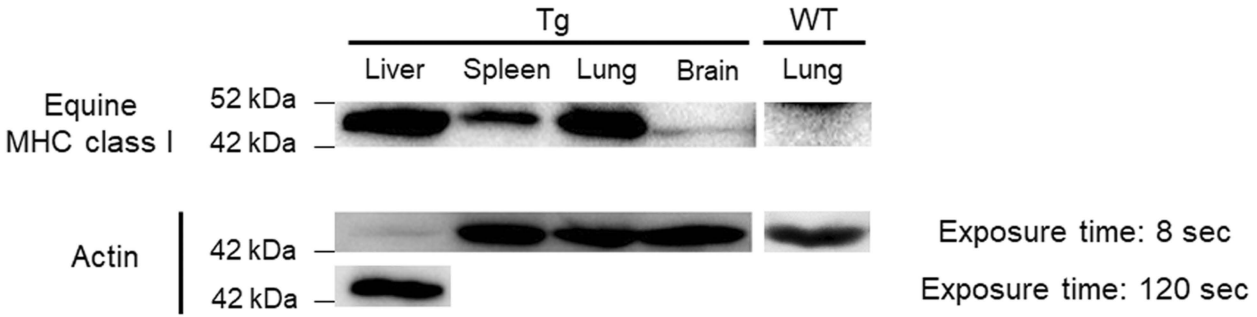
Tg
WT
Liver
Spleen
Lung
Brain
Lung
Equine
MHC class I
52 kDa
42 kDa
Actin
42 kDa
42 kDa
Exposure time: 8 sec
Exposure time: 120 sec

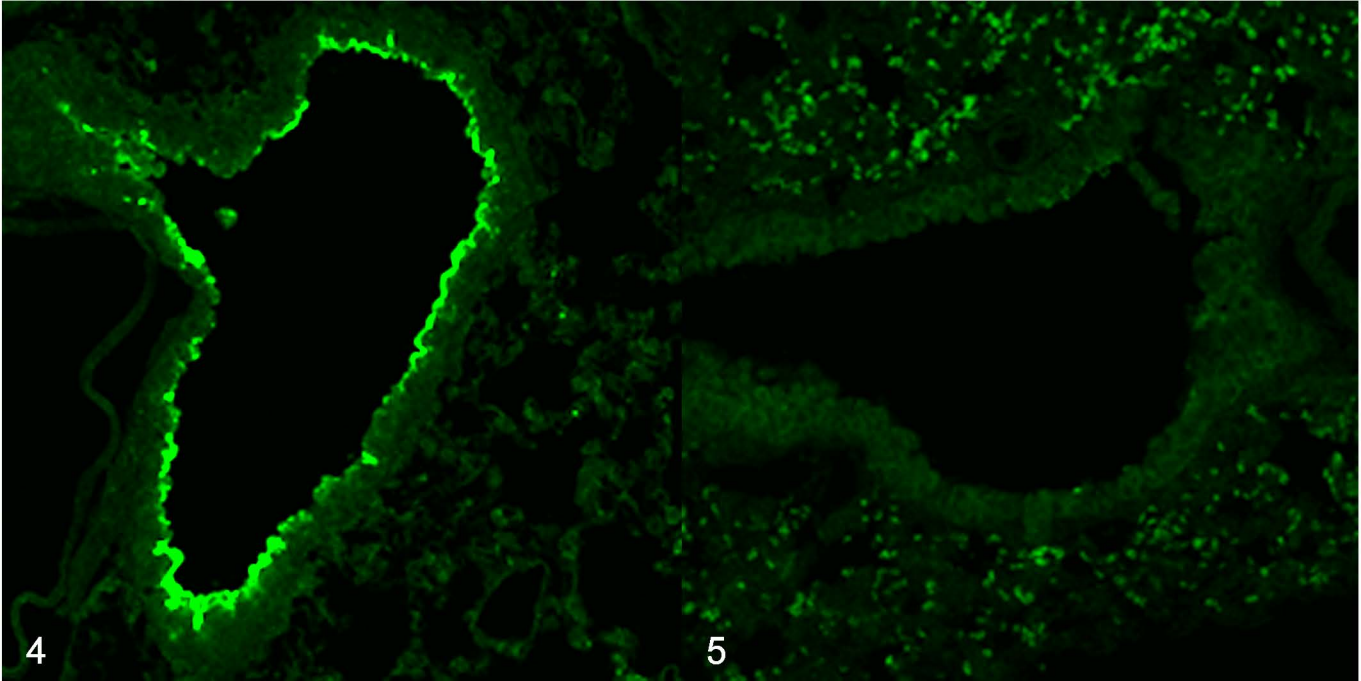
4
5

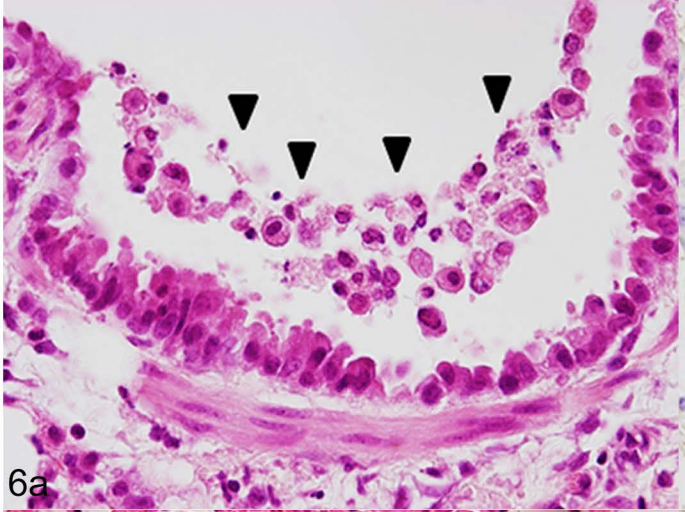

6a

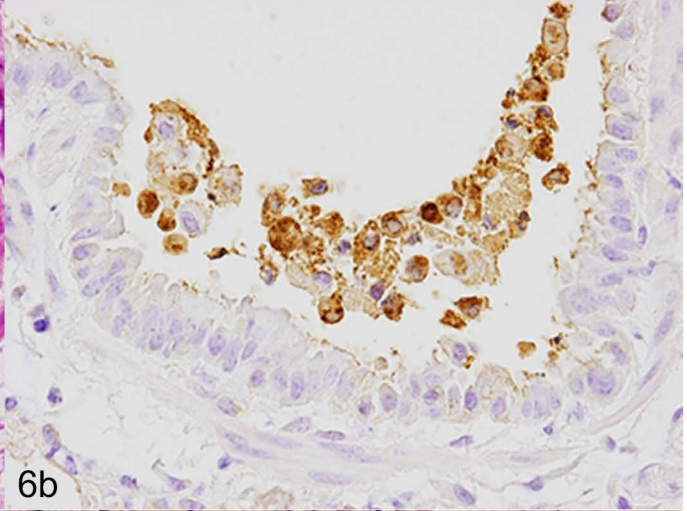

6b

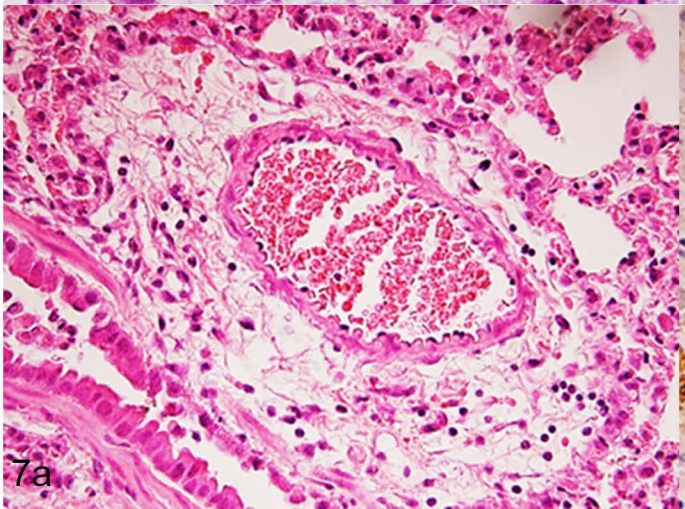

7a

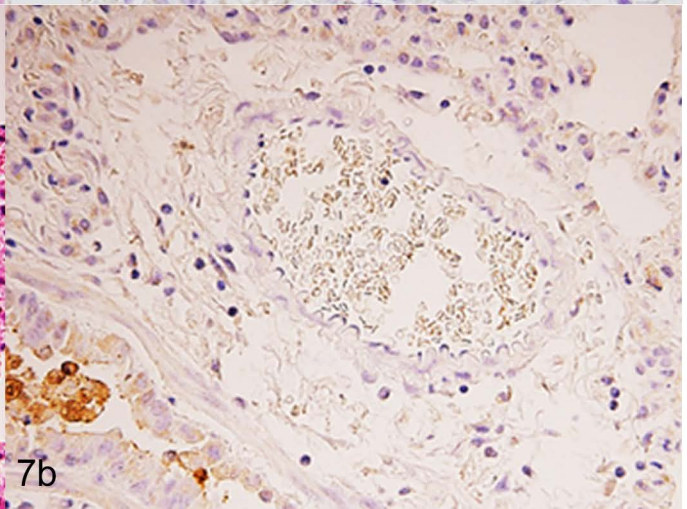

7b

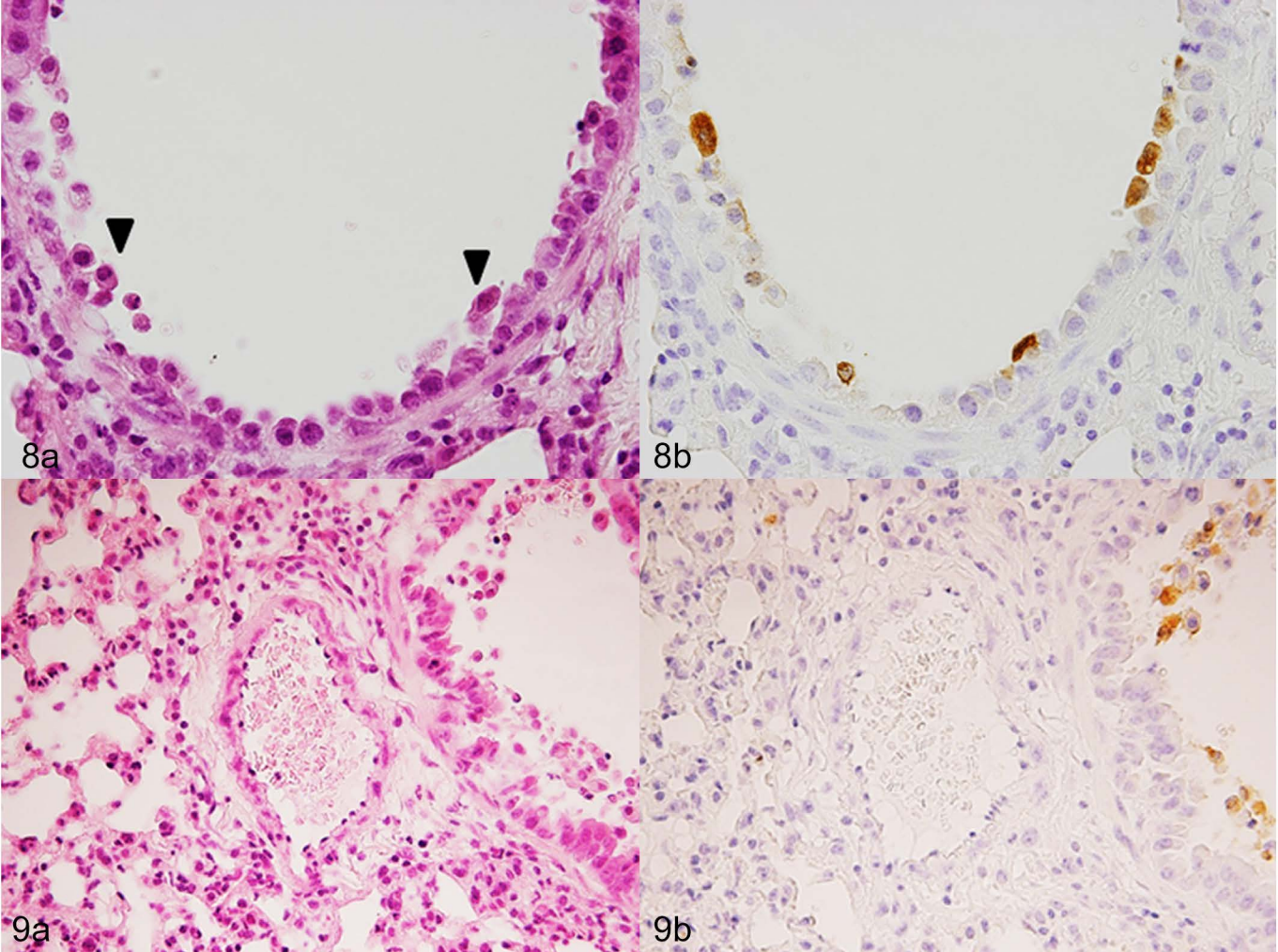
8a
8b
9a
9b

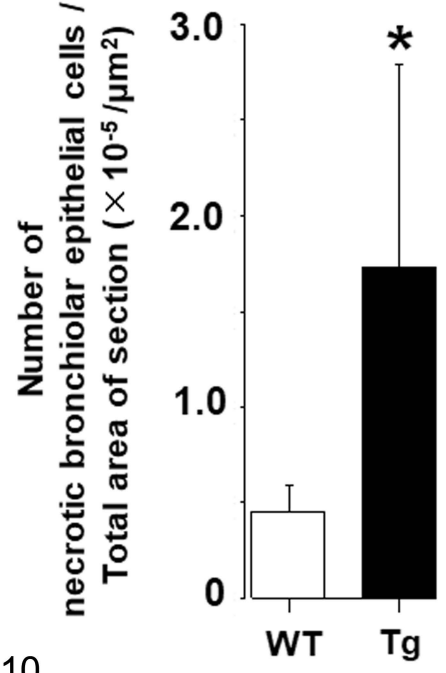
Number of necrotic bronchiolar epithelial cells / Total area of section (×10-5/μm2)
3.0
2.0
1.0
0
*
WT
Tg

10

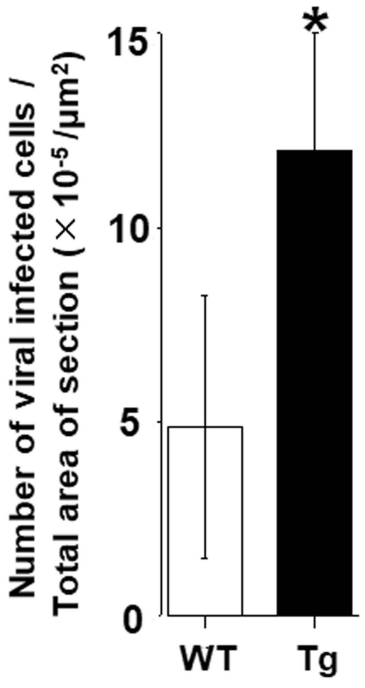
Number of viral infected cells / Total area of section (×10-5/μm2)
15
10
5
0
*
WT
Tg

11

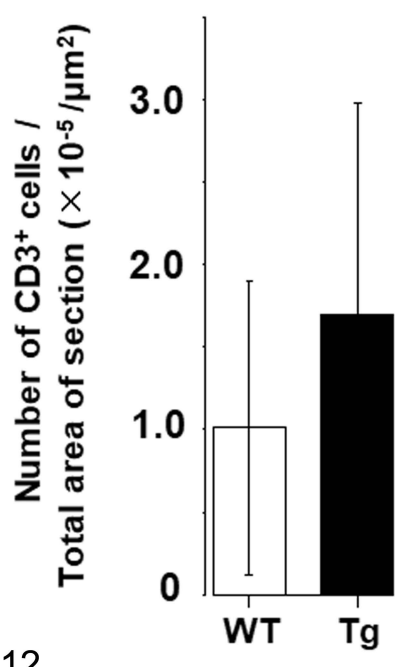
Number of CD3+ cells / Total area of section (×10-5/μm2)
3.0
2.0
1.0
0
WT
Tg

12